

Forecasting range shifts of a dioecious plant species under climate change

Jacob K. Moutouama ^{*1}, Aldo Compagnoni², and Tom E.X. Miller¹

¹Program in Ecology and Evolutionary
Biology, Department of BioSciences, Rice University, Houston, TX USA

²Institute
of Biology, Martin Luther University Halle-Wittenberg, Halle, Germany; and
German Centre for Integrative Biodiversity Research (iDiv), Leipzig, Germany

Running header: Forecasting range shifts

Keywords: climate change, demography, forecasting, matrix projection model, mechanistic models, sex ratio, range limits

Acknowledgements: This research was supported by XX.

Authorship statement: XXXXX.

Data accessibility statement: All data (Miller and Compagnoni, 2022a) used in this paper are publicly available. Should the paper be accepted, all computer scripts supporting the results will be archived in a Zenodo package, with the DOI included at the end of the article. During peer review, our data and code are available at <https://github.com/jmoutouama/POAR-Forecasting>.

Conflict of interest statement: None.

^{*}Corresponding author: jmoutouama@gmail.com

1 Abstract

2 Rising temperatures and extreme drought events associated with global climate change have
3 triggered an urgent need for predicting species response to climate change. Currently, the
4 vast majority of theory and models in population biology, including those used to forecast
5 biodiversity responses to climate change, ignore the complication of sex structure. To address
6 this issue, we developed a climate-driven population matrix model using demographic data of
7 dioecious species (Texas bluegrass), past and future climate (different gas emission scenarios)
8 to forecast and backcast the effect of climate change on range shifts. Our results show a sex
9 specific demographic response to climate change. Female individuals have a demographic
10 advantage (higher vital rate) over males. Female demographic advantage led to a slight decline
11 in population viability under future climate assuming moderate gas emission and a drastic
12 reduction in population viability under future climate assuming high gas emission. Despite
13 a change in species range, climate change will likely alter population viability in dioecious
14 species. Overall, our work suggest that tracking only the female could lead to a slight overesti-
15 mation of the impact of climate change on dioecious species. This study provides a framework
16 for predicting the impact of climate on dioecious species using population demography.

¹⁷ Introduction

¹⁸ Rising temperatures and extreme drought events associated with global climate change are
¹⁹ leading to increased concern about how species will become redistributed across the globe
²⁰ under future climate conditions (Bertrand et al., 2011; Gamelon et al., 2017; Smith et al., 2024).
²¹ Dioecious species (most animals and many plants) might be particularly vulnerable to the
²² influence of climate change because they often display skewed sex ratios that are generated or
²³ reinforced by sexual niche differentiation (distinct responses of females and males to shared cli-
²⁴ mate drivers) (Tognetti, 2012). Accounting for such a niche differentiation within a population
²⁵ is a long-standing challenge in accurately predicting which sex will successfully track environ-
²⁶ mental change and how this will impact population viability and range shifts (Gissi et al., 2023;
²⁷ Jones et al., 1999). The vast majority of theory and models in population biology, including
²⁸ those used to forecast biodiversity responses to climate change, ignore the complication of sex
²⁹ structure (Ellis et al., 2017; Pottier et al., 2021). As a result, accurate forecasts of colonization-
³⁰ extinction dynamics for dioecious species under future climate scenarios are limited.

³¹ Species's range limits, when not driven by dispersal limitation, should generally reflect
³² the limits of the ecological niche (Lee-Yaw et al., 2016). For most species, niches and geographic
³³ ranges are often limited by climatic factors including temperature and precipitation (Sexton
³⁴ et al., 2009). Therefore, any substantial changes in the magnitude of these climatic factors in a
³⁵ given location across the range could impact population viability, with implications for range
³⁶ shifts based on which regions become more or less suitable (Davis and Shaw, 2001; Pease
³⁷ et al., 1989). Forecasting range shifts for dioecious species is complicated by the potential for
³⁸ each sex to respond differently to climate variation (Morrison et al., 2016; Pottier et al., 2021).
³⁹ Populations in which males are rare under current climatic conditions could experience low
⁴⁰ reproductive success due to sperm or pollen limitation that may lead to population decline in
⁴¹ response to climate change that disproportionately favors females (Eberhart-Phillips et al., 2017).
⁴² In contrast, climate change could expand male habitat suitability (e.g. upslope movement),
⁴³ which might increases seed set for pollen-limited females and favor range expansion (Petry
⁴⁴ et al., 2016). Although the response of species to climate warming is an urgent and active area
⁴⁵ of research, few studies have disentangled the interaction between sex and climate drivers
⁴⁶ to understand their combined effects on population dynamics and range shifts.

⁴⁷ Our ability to track the impact of climate change on the population dynamics of
⁴⁸ dioecious plants and the implication of such impact on range shift depends on our ability
⁴⁹ to build mechanistic models that take into account the spatial and temporal context in which
⁵⁰ sex specific response to climate change affects population viability (Czachura and Miller, 2020;
⁵¹ Davis and Shaw, 2001; Evans et al., 2016). For example, structured models that are built from

52 long-term demographic data collected from common garden experiments have emerged as
53 powerful technic to study the impact of climate change on species range shift (Merow et al.,
54 2017; Schwinnig et al., 2022). These structured models are increasingly utilized for two
55 reasons. First, they enable the manipulation of treatments that can isolate spatial and temporal
56 correlations between environmental factors, thus overcoming a main disadvantage with many
57 types of correlative studies (Leicht-Young et al., 2007). Second, they link individual-level
58 demographic trait to population demography allowing the investigation of the demographic
59 mechanisms behind vital rates (e.g. survival,fertility, growth and seed germination) response
60 environmental variation (Dahlgren et al., 2016; Louthan et al., 2022). Third, these structured
61 models can be used to identify which aspect of climate is more important for population
62 dynamics. For example, Life Table Response Experiment (LTRE) build from structured
63 models is an approach that has become widely used to understand how a given treatment
64 (eg. temperature or precipitation) could affect population dynamics (Caswell, 1989; Iler et al.,
65 2019; Morrison and Hik, 2007; O'Connell et al., 2024).

66 In this study, we used a mechanistic approach by combining geographically-distributed
67 field experiments, hierarchical statistical modeling, and two-sex population projection
68 modeling to understand the demographic response of dioecious species to climate change and
69 its implications for future range dynamics. Our study system is a dioecious plant species (*Poa*
70 *arachnifera*) distributed along environmental gradients in the south-central US corresponding
71 to variation in temperature across latitude and precipitation across longitude. A previous
72 study on the same system showed that, despite a differentiation of climatic niche between
73 sexes, the female niche mattered the most in driving the environmental limits of population
74 viability (Miller and Compagnoni, 2022b). However that study did not use climate variables
75 preventing us from backcasting and forecasting the impact of climate change on dioecious
76 species. Here, we asked four questions:

- 77 1. What are the sex-specific vital rate responses to variation in temperature and precipitation
78 across the species' range ?
- 79 2. How sex-specific vital rates combine to determine the influence of climate variation on
80 population growth rate (λ) ?
- 81 3. What are the historical and projected changes in climate across the species range ?
- 82 4. What are the back-casted and fore-casted dynamics of this species' geographic niche
83 ($\lambda \geq 1$) and how does accounting for sex structure modify these predictions ?

⁸⁴ **Materials and methods**

⁸⁵ **Study species**

⁸⁶ Texas bluegrass (*Poa arachnifera*) is a dioecious perennial, summer-dormant cool-season (C3)
⁸⁷ grass that occurs in the south-central U.S. (Texas, Oklahoma, and southern Kansas) (Hitchcock,
⁸⁸ 1971). Average temperatures along the distribution of the species tend to decrease northward
⁸⁹ as a result of the influence of latitude: lower latitudes receive more heat from the sun over
⁹⁰ the course of a year. Similarly the average precipitation decrease eastward as a result of
⁹¹ the influence of longitude: lower longitudes receive less precipitation over the year. Texas
⁹² bluegrass grows between October and May (growing season), with onset of dormancy often
⁹³ from June to September (dormant season) (Kindiger, 2004). Flowering occurs in May and
⁹⁴ the species is wind pollinated (Hitchcock, 1971).

⁹⁵ **Common garden experiment**

⁹⁶ We set up a common garden experiment throughout and beyond the range of Texas bluegrass
⁹⁷ to enable study of sex-specific demographic responses to climate and the implications for range
⁹⁸ shifts. The novelty of this study lies in the fact that we use a precise climate variable to build
⁹⁹ a mechanistic model to forecast the response of species to climate change. Details of the exper-
¹⁰⁰ imental design are provided in Miller and Compagnoni (2022b); we provide a brief overview
¹⁰¹ here. The common experiment was installed at 14 sites across a climatic gradient (Fig.1. At
¹⁰² each site, we established 14 blocks. For each block we planted three female and three male indi-
¹⁰³ viduals that were clonally propagated from eight natural source populations of Texas bluegrass.
¹⁰⁴ The experiment was established in November 2013 and was census annually through 2016, pro-
¹⁰⁵ viding both spatial and inter-annual variation in climate. Each May (2014-2016), we collected
¹⁰⁶ individual demographic data including survival (alive or dead), growth (number of tillers),
¹⁰⁷ flowering status (reproductive or vegetative), and fertility (number of panicles, conditional on
¹⁰⁸ flowering). For the analyses that follow, we focus on the 2014-15 and 2015-16 transitions years.

¹⁰⁹ **Climatic data collection**

¹¹⁰ We downloaded monthly temperature and precipitation from Chelsa to describe observed
¹¹¹ climate conditions during our study period (Karger et al., 2017). These climate data were used
¹¹² as covariates in vital rate regressions, which allowed us to forecast and back-cast demographic
¹¹³ responses to climate change based on observations across the common garden experiment.

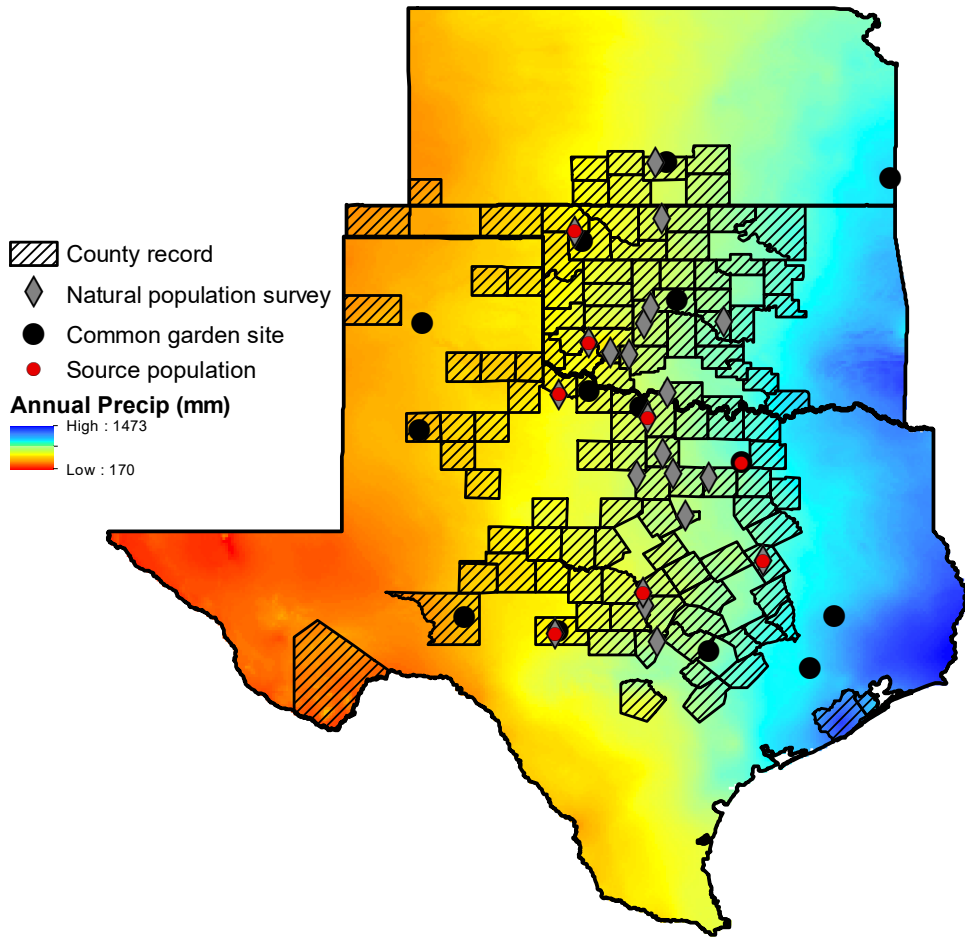


Figure 1: XXX

114 We aligned the climatic years to match demographic transition years (**May 1 – April 30**)¹
 115 rather than calendar years. Based on the natural history of this summer-dormant cool-season
 116 species, we divided each transition year into growing and dormant seasons. We define June
 117 through September as the dormant season and the rest of the year as the growing season.
 118 Across years and sites, the experiment included substantial variation in growing and dormant
 119 season temperature and precipitation (Supporting Information S-1, S-2).

120 To back-cast and forecast changes in climate, we downloaded projection data for three
 121 30-year periods: past (1901-1930), current (1990-2019) and future (2070-2100). Data for these
 122 climatic periods were downloaded from four general circulation models (GCMs) selected
 123 from the Coupled Model Intercomparison Project Phase 5 (CMIP5). The GCMs are MIROC5,
 124 ACCESS1-3, CESM1-BGC, CMCC-CM and were downloaded from chelsa (Sanderson

¹I am not sure if these are actually the right dates.

¹²⁵ et al., 2015). We evaluated future climate projections from two scenarios of representative
¹²⁶ concentration pathways (RCPs): RCP4.5, an intermediate-to-pessimistic scenario assuming
¹²⁷ a radiative forcing to amount to 4.5 Wm^{-2} by 2100, and RCP8.5, a pessimistic emission
¹²⁸ scenario which project a radiative forcing to amount to 8.5 Wm^{-2} by 2100 (Schwalm et al.,
¹²⁹ 2020; Thomson et al., 2011).

¹³⁰ Sex ratio experiment

¹³¹ We conducted a sex-ratio experiment on a site close (1 km) to a natural population of the
¹³² focal species at the center of the range to estimate the effect of sex-ratio variation on female
¹³³ reproductive success. Details of the experiment are provided in Compagnoni et al. (2017) and
¹³⁴ Miller and Compagnoni (2022b). In short, we established 124 experimental populations on
¹³⁵ plots measuring $0.4 \times 0.4\text{m}$ and separated by at least 15m from each other at that site. We chose
¹³⁶ 15m because our pilot data show that more than 90% of wind pollination occurred within 13m.
¹³⁷ We varied population density (1-48 plants/plot) and sex ratio (0%-100% female) across the ex-
¹³⁸ perimental populations, and we replicated 34 combinations of density-sex ratios. We collected
¹³⁹ the number of panicles from a subset of females in each plot and collected the number of
¹⁴⁰ seeds in each panicle. Since the number of panicles (proxy of reproduction effort) does not nec-
¹⁴¹ essarily reflect reproduction success in *Poar arachnifera*, we accessed reproduction success (seed
¹⁴² fertilized) using greenhouse-based germination and trazolium-based seed viability assays.

¹⁴³ We used the sex-ratio to estimate the probability of viability and the germination rate.
¹⁴⁴ Seed viability was modeled with a binomial distribution where the probability of viability
¹⁴⁵ (v) was given by:

$$\sup{146} v = v_0 * (1 - OSR^\alpha) \quad (1)$$

¹⁴⁷ where OSR is the operational sex ratio (proportion of panicles that were female) in the
¹⁴⁸ experimental populations. The properties of the above function is supported by our previous
¹⁴⁹ work (Compagnoni et al., 2017). Here, seed viability is maximized at v_0 as OSR approaches
¹⁵⁰ zero (strongly male-biased) and goes to zero as OSR approaches 1 (strongly female-biased).
¹⁵¹ Parameter α controls how viability declines with increasing female bias.

¹⁵² We used a binomial distribution to model the germination data from greenhouse trials.
¹⁵³ Given that germination was conditional on seed viability, the probability of success was given
¹⁵⁴ by the product $v * g$, where v is a function of OSR (Eq. 1) and g is assumed to be constant.

155 **Sex specific demographic responses to climate**

156 We used individual level measurements of survival, growth (number of tillers), flowering, num-
157 ber of panicles to independently develop Bayesian mixed effect models describing how each
158 vital rate varies as a function of sex, size, precipitation of growing and dormant season and tem-
159 perature of of growing and dormant season. We fit vital rate models with second-degree poly-
160 nomial functions for the influence of climate. We included a second-degree polynomial because
161 we expected that climate variables would affect vital rates through a hump-shaped relationship.

162 We centered and standardized all climatic predictors to facilitate model convergence.
163 However, Size was on a natural logarithm scale. We included site,source, and block as
164 random effect. All the vital rate models used the same linear and quadratic predictor for
165 the expected value (μ)(Eq.2) . However, we applied a different link function ($f(\mu)$) depending
166 on the distribution the vital rate. We modeled survival and flowering data with a Bernoulli
167 distribution. We modeled the growth (tiller number) with a zero-truncated Poisson inverse
168 Gaussian distribution. Fertility (panicle count) was model as zero-truncated negative binomial.

$$f(\mu) = \beta_0 + \beta_1 size + \beta_2 sex + \beta_3 pptgrow + \beta_4 pptdorm + \beta_5 tempgrow + \beta_6 tempdorm + \beta_7 pptgrow * sex + \beta_8 pptdorm * sex + \beta_9 tempgrow * sex + \beta_{10} tempdorm * sex + \beta_{11} size * sex + \beta_{12} pptgrow * tempgrow + \beta_{13} pptdorm * tempdorm + \beta_{14} pptgrow * tempgrow * sex + \beta_{15} pptdorm * tempdorm * sex + \beta_{16} pptgrow^2 + \beta_{17} pptdorm^2 + \beta_{18} tempgrow^2 + \beta_{19} tempdorm^2 + \beta_{20} pptgrow^2 * sex + \beta_{21} pptdorm^2 * sex + \beta_{22} tempgrow^2 * sex + \beta_{23} tempdorm^2 * sex + \phi + \rho + \nu \quad (2)$$

170 where β_0 is the grand mean intercept, β_1 is the size dependent slopes. *size* was on a natural log-
171 arithm scale. $\beta_2 \dots \beta_{13}$ represent the climate dependent slopes. $\beta_{14} \dots \beta_{23}$ represent the sex-climate
172 interaction slopes. *pptgrow* is the precipitation of the growing season (standardized to mean
173 zero and unit variance), *tempgrow* is the temperature of the growing season (standardized to
174 mean zero and unit variance), *pptdorm* is the precipitation of the dormant season (standardized
175 to mean zero and unit variance), *tempdorm* is the temperature of the dormant season (standard-
176 ized to mean zero and unit variance). The model also includes normally distributed random ef-
177 fects for block-to-block variation ($\phi \sim N(0, \sigma_{block})$) and source-to-source variation that is related
178 to the provenence of the seeds used to establish the common garden ($\rho \sim N(0, \sigma_{source})$), site to
179 site variation ($\nu \sim N(0, \sigma_{site})$). We fit survival, growth, flowering models with generic weakly in-
180 formative priors for coefficients ($\mu = 0, \sigma = 1.5$) and variances ($\gamma[0.1, 0.1]$). **We fit fertility model**
181 **with regularizing priors for coefficients ($\mu = 0, \sigma = 0.15$)**. We ran three chains for 1000 samples
182 for warmup and 4000 for interactions, with a thinning rate of 3. We accessed the quality of the

models using trace plots and predictive check graphs (Piironen and Vehtari, 2017) (Supporting Information S-4). To understand the effect of climate on vital rates, we got the 95 % credible interval of the posterior distribution. Then we assumed that there is 95 % probability that the true (unknown) estimates would lie within that interval, given the evidence provided by the observed data for each vital rate. All models were fit in Stan (Stan Development Team, 2023).

Influence of climate variation on population growth rate

To understand the effect of climate on population growth rate, we used the vital rate estimated earlier to build a matrix projection model (MPM) structured by size (number of tillers), sex and climate (dormant and growing) as covariate. Let $F_{x,z,t}$ and $M_{x,z,t}$ be the number of female and male plants of size x in year t present at a location that has z as climate, where $x \in \{1, 2, \dots, U\}$ and U is the maximum number of tillers a plant can reach (here 95th percentile of observed maximum size). Let F_t^R and M_t^R be the new recruits, which we assume do not reproduce in their first year. We assume that the parameters of sex ratio-dependent mating (Eq. 1) do not vary with climate. For a pre-breeding census, the expected numbers of recruits in year $t+1$ is given by:

$$F_{t+1}^R = \sum_{x=1}^U [p^F(x,z) \cdot c^F(x,z) \cdot d \cdot v(\mathbf{F}_t, \mathbf{M}_t) \cdot m \cdot \rho] F_{x,z,t} \quad (3)$$

$$M_{t+1}^R = \sum_{x=1}^U [p^F(x,z) \cdot c^F(x,z) \cdot d \cdot v(\mathbf{F}_t, \mathbf{M}_t) \cdot m \cdot (1-\rho)] F_{x,z,t} \quad (4)$$

where p^F and c^F are flowering probability and panicle production for females of size x , d is the number of seeds per female panicle, v is the probability that a seed is fertilized, m is the probability that a fertilized seed germinates, and ρ is the primary sex ratio (proportion of recruits that are female), z is the climate. Seed fertilization depends on the OSR of panicles (following Eq. 1) which was derived from the $U \times 1$ vectors of population structure \mathbf{F}_t and \mathbf{M}_t :

$$v(\mathbf{F}_t, \mathbf{M}_t) = v_0 * \left[1 - \left(\frac{\sum_{x=1}^U p^F(x,z) c^F(x,z) F_{x,z,t}}{\sum_{x=1}^U p^F(x,z) c^F(x,z) F_{x,z,t} + p^M(x,z) c^M(x,z) M_{x,z,t}} \right)^\alpha \right] \quad (5)$$

Thus, the dynamics of the size-structured component of the population are given by:

$$F_{y,t+1} = [\sigma \cdot g^F(y, x=1, z)] F_t^R + \sum_{x=1}^U [s^F(x,z) \cdot g^F(y, x, z)] F_{x,z,t} \quad (6)$$

$$M_{y,t+1} = [\sigma \cdot g^M(y, x=1, z)] M_t^R + \sum_{x=1}^U [s^M(x,z) \cdot g^M(y, x, z)] M_{x,z,t} \quad (7)$$

209 In the two formula above, the first term indicates seedlings that survived their first year and en-
 210 ter the size distribution of established plants. Instead of using *P. arachnifera* survival probability,
 211 we used the seedling survival probability (σ) from demographic studies of the hermaphroditic
 212 congener *Poa autumnalis* in east Texas (T.E.X. Miller and J.A. Rudgers, *unpublished data*), and we
 213 assume this probability was constant across sexes and climatic variables. We did this because
 214 we had little information on the early life cycle transitions of greenhouse-raised transplants.
 215 We also assume that $g(y, x = 1)$ is the probability that a surviving seedlings reach size y ,
 216 the expected future size of 1-tiller plants from the transplant experiment. The second term
 217 represents survival and size transition of established plants from the previous year, where
 218 s and g give the probabilities of surviving at size x and growing from sizes x to y , respectively,
 219 and superscripts indicate that these functions may be unique to females (F) and males (M).

220 Since the two-sex MPM is nonlinear (vital rates affect and are affected by population
 221 structure) we estimated the asymptotic geometric growth rate (λ) by numerical simulation,
 222 and repeated this across a range of climate.

223 Identifying the mechanisms of population growth rate sensitivity to climate

224 To identify which aspect of climate is most important for population viability, we used
 225 a "random design" Life Table Response Experiment (LTRE). We used the RandomForest
 226 package to fit a regression model with θ as predictors and λ_c as response (Ellner et al., 2016;
 227 Liaw et al., 2002). The LTRE approximates the variation in λ in response to climate covariates
 228 and their interaction (Caswell, 2000; Hernández et al., 2023):

$$229 \quad Var(\lambda_c) \approx \sum_{i=-1}^n \sum_{j=1}^n Cov(\theta_i, \theta_j, \theta_{ij}) + Var(\epsilon) \quad (8)$$

230 where, θ_i , θ_j , θ_{ij} represent respectively the fitted regression slope for the covariate of the
 231 dormant season, j the covariate of the growing season and ij the covariate of their interactions.

232 Because LTRE contributions are additive, we summed across vital rates to compare the
 233 total contributions of female and male parameters.

234 Impact of climate change on niche and range shifts

235 A species' ecological niche can be defined as the range of resources and conditions (physical
 236 and environmental) allowing the species to maintain a viable population ($\lambda \geq 1$). To
 237 understand the impact of climate change on species niche shifts, we estimated the probability
 238 of population viability being greater than 1, $Pr(\lambda > 1)$ conditional to two environmental
 239 axes (Diez et al., 2014). Because the study species is a cool season grass species, we used

240 two environmental axes: (1) temperature and precipitation of the dormant season and (2)
241 temperature and precipitation of the growing season. $\text{Pr}(\lambda > 1)$ was calculated using the
242 proportion of the Markov chain Monte Carlo iterations (here, 300) that lead to a $\lambda > 1$
243 Population viability-environment relationship was mapped onto geographic layers of three
244 state (Texas, Oklahoma and Kansas) to delineate past, current and future potential distribution
245 of the species. To do so, we estimated $\text{Pr}(\lambda > 1)$ as a function of all climate covariates for
246 each pixel (1km*1km) across the species range using the posterior distribution. Because of
247 amount of the computation involve in the Markov chain Monte Carlo iterations, use only
248 100 posterior samples to estimate $\text{Pr}(\lambda > 1)$ across the Texas, Oklahoma and Kansas.

249 All the analysis were performed in R 4.3.1 (R Core Team, 2023)

250 Results

251 Sex specific demographic response to climate change

252 Most vital rates were strongly climate dependent, but the magnitude of their response
253 differed between sexes suggesting a sex-specific demographic response to climate. Survival
254 and flowering were strongly more dependent on climate than growth (number of tillers) and
255 reproduction (number of panicles) (Fig.2; Supporting Information S-5). In addition, we found
256 opposite patterns in the direction of the effect on seasonal climate on the probability of survival
257 and flowering. The growing season (precipitation) has a negative effect on the probability of
258 survival, number of tillers, and the probability of flowering, whereas the dormant season has
259 a positive effect on these vital rates. Unlike precipitation, temperature had different effects on
260 different vital rates. Temperature of the growing season has a positive effect of the probability
261 of survival, a negative effect of the probability of flowering, and the number of tillers, but no
262 significant effect on the number of panicles. Further, there was a female survival and flowering
263 advantage across both climatic seasons (Figures. 3A-3D, 3I-3L). On the contrary, there was
264 a male panicle advantage across all climatic variables (Figure3M-3P). Counter-intuitively, there
265 was no significant sex growth advantage in all season climatic variables (Figures. 3E-3H).
266 Plant size x sex interaction was significant for all vitals rates (Supporting Information S-5). For
267 survival, flowering and reproduction the interaction between temperature and precipitation
268 of the growing season and dormant season was not significant (Supporting Information S-5).
269 However, for growth the interaction between temperature and precipitation of the growing
270 season and dormant season was significantly higher than zero (Supporting Information S-5).

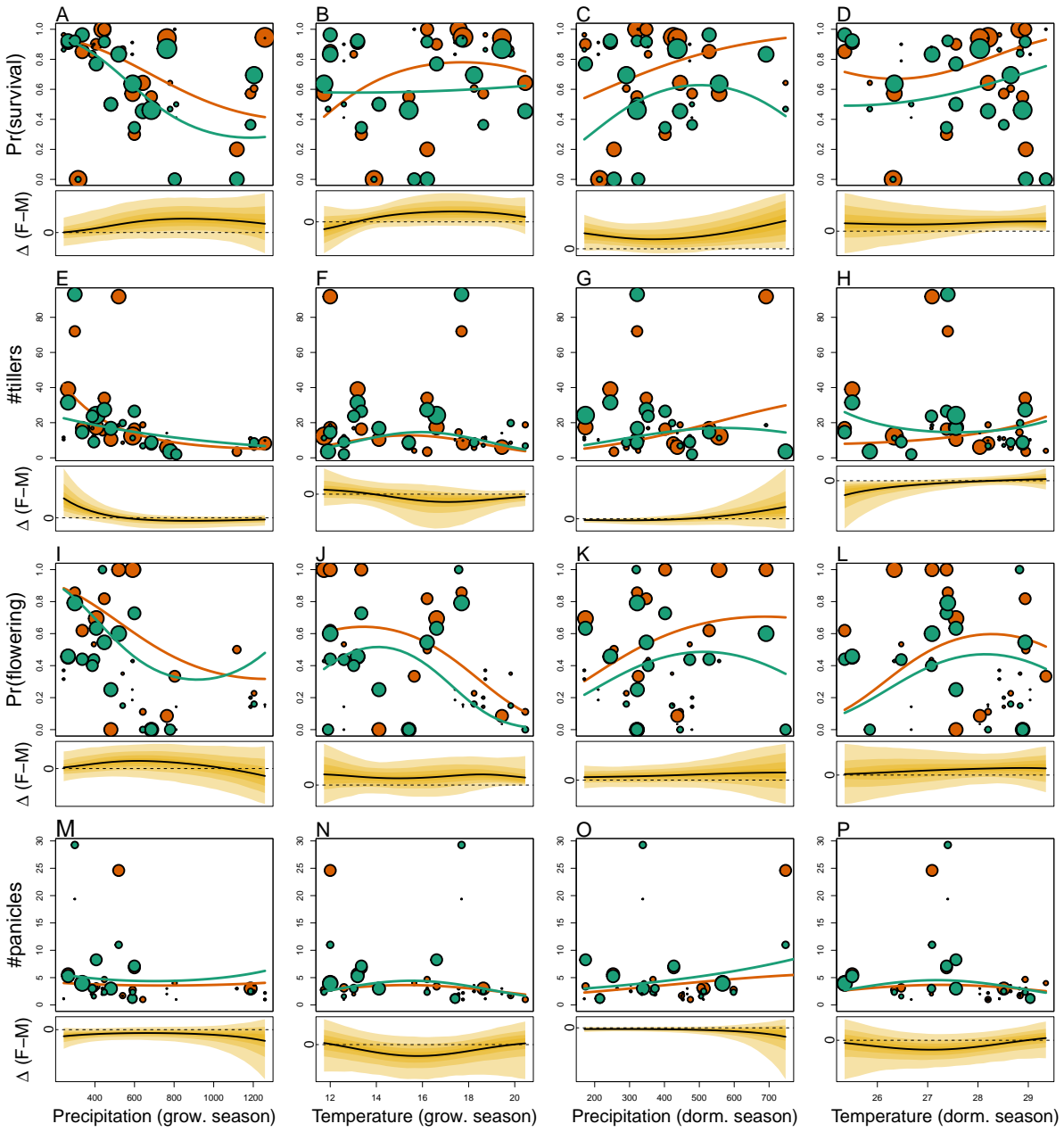


Figure 2: Sex specific demographic response to climate across species range: A–D, inter-annual probability of survival; E–H, inter-annual growth (change in number of tillers); I–L, probability of flowering; M–P, number of panicles produced given flowering. Points show means by site for females (orange) and males (green). Point size is proportional to the sample size of the mean. Lines show fitted statistical models for females (orange) and males (green) based on posterior mean parameter values. Lower panels below each data panel show the posterior distribution of the difference between females and males as a function of climate (positive and negative values indicate female and male advantage, respectively); dashed horizontal line shows zero difference.

271 Climate change alter population viability

272 We estimated the predicted response of population growth rate (population fitness) to
 273 seasonal climate gradients using a model assuming a female dominant model and another

model using the two sexes. Consistent with the effect of climate on the individual vital rate, we found a strong effect of seasonal climate on population fitness (Fig.3). For both models (female dominant and two sexes), population fitness decreased with an increase of precipitation of growing season. In contrast population fitness increased with precipitation of the dormant season. Furthermore, population fitness was maximized between 23 and 17 °C and decreases to zero just beyond 32 °C during the growing season. Similarly population fitness was maximized between 13 and 17 °C and decreases to zero just beyond 20 °C during the growing season. We have also detected a strong effect of the past and future climate on population growth rate. However, for future climate, the magnitude of that effect was different between gas-scenario emissions. A moderate emission gas scenario (RCP4.5) has a no effect on the population growth rate while a high emission scenario (RCP8.5) has a strong negative effect on the population growth rate. High-emission scenario (RCP8.5) will lead to an alteration of population viability. Under past climate conditions, population growth rate decreased below one for temperature of the growing season and the dormant season.

288 Climatic change induce range shifts

289 Across species niche population persistence was maximized at higher temperature during the
290 dormant season (27 to 31) and intermediate temperature during the growing season (11 to
291 20). Our demographically based range predictions broadly captured the known distribution
292 of the species (Fig. 1). More specifically, the predicted population viable ($\lambda > 1$) matches
293 the presence and absence of the species. Furthermore, viable populations of *P. arichnifera*
294 were only predicted at the center of the range for current climatic conditions (Fig1). Future
295 and past projections of climate change showed a north-west range shift compared to current
296 distributions. Although *P. arichnifera* was predicted to have suitable habitat in the center of the
297 range under the current climate, future warming is predicted to reduce much of the suitable
298 habitat in the southern part (Figure).

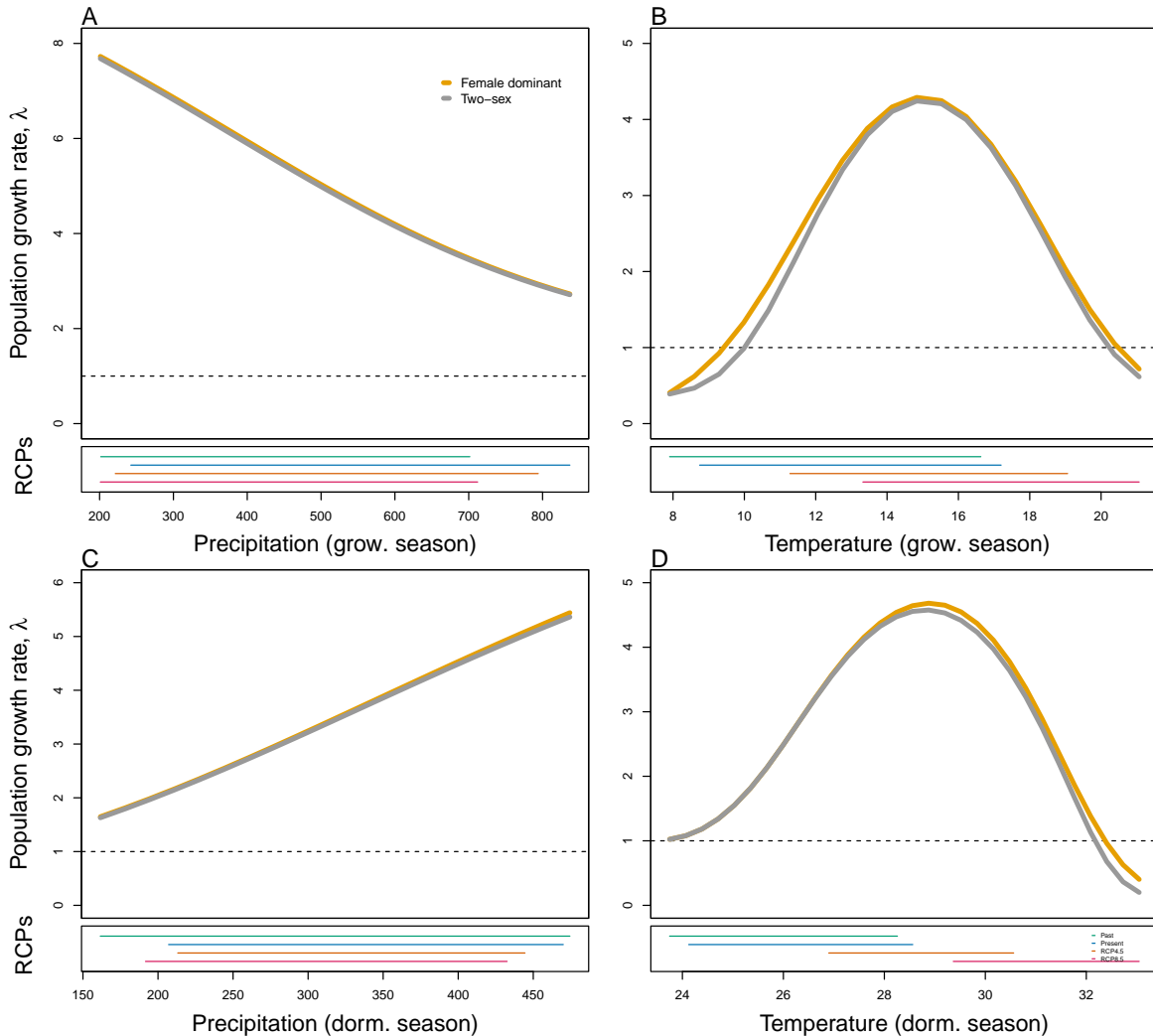


Figure 3: Population growth rate (λ) as a function of climate (past climate, present and predicted future climates). For future climate, we show a Representation Concentration Pathways 4.5 and 8.5. Values of (λ) are derived from the mean climate variables across 4 GCMs. The solid bold curve shows prediction by the two-sex matrix projection model that incorporates sex- specific demographic responses to climate with sex ratio dependent seed fertilization. The bold dashed curve represents the prediction by the female dominant matrix projection model. The dashed horizontal line indicates the limit of population viability ($\lambda = 1$)

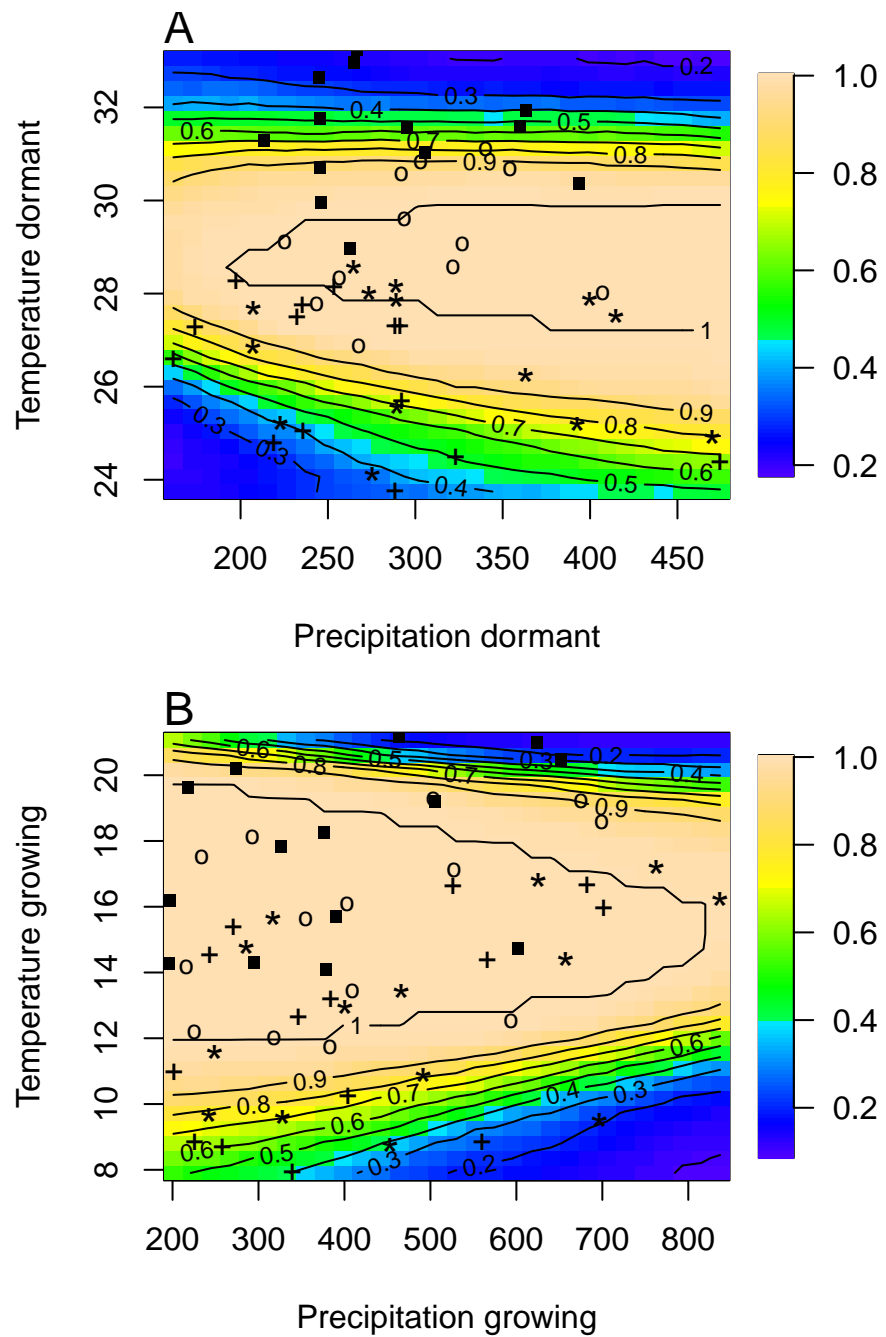


Figure 4: Predicted niche shift for past, present and future climate conditions based on $\text{Pr} (\lambda \geq 1)$. Niche of dormant season (A), Niche of growing season (B). Contours show predicted probabilities of self-sustaining populations $\text{Pr} (\lambda \geq 1)$ conditional on precipitation and temperature of the dormant and growing season. "+" Past, "*" Current, "o" RCP 45, "." RCP 85

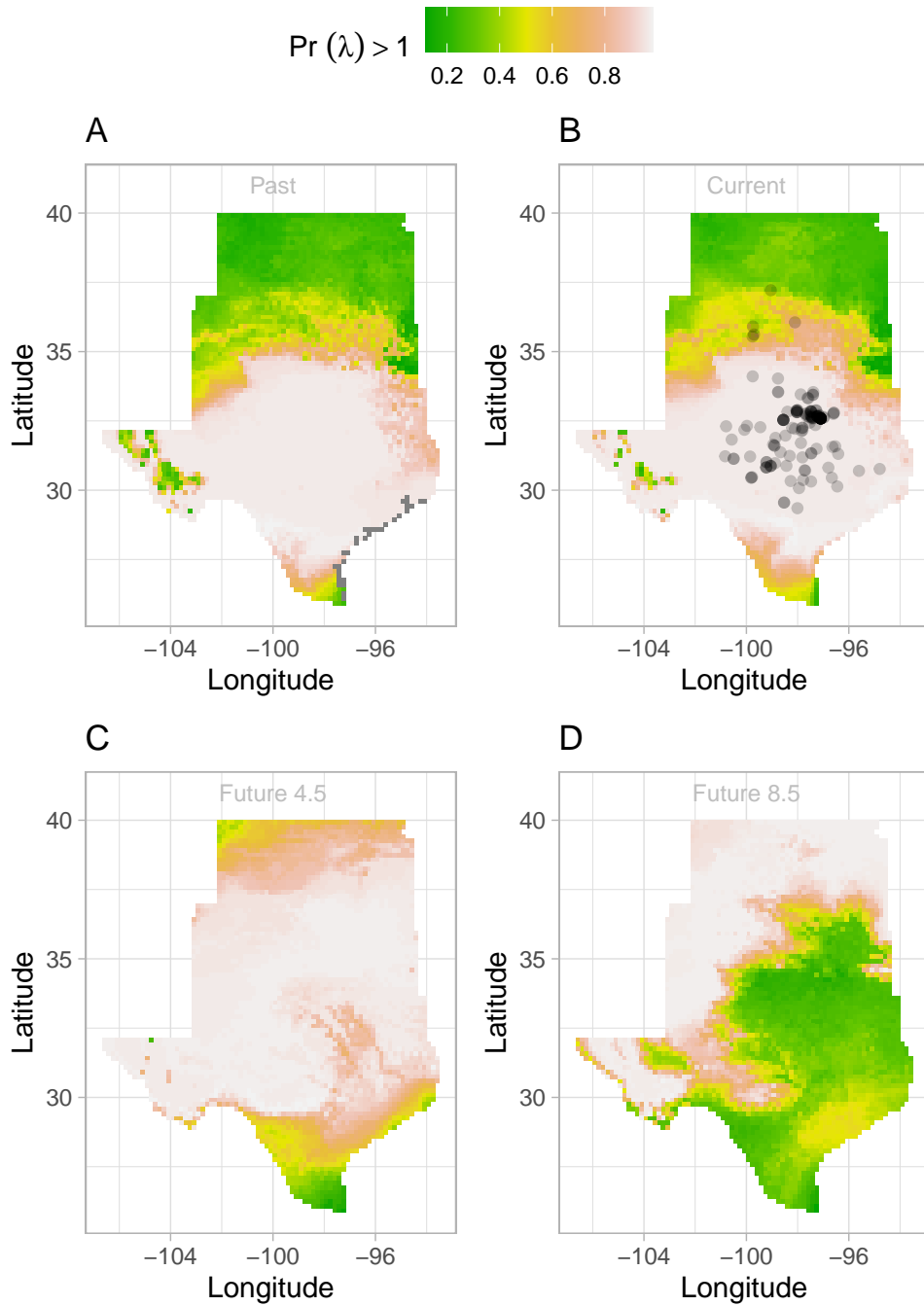


Figure 5: Past (A), Current (B), Future (2070–20100) (C and D) predicted range shift based on population growth rate. Future projections were based on the average population growth rate in four GCMs. The black circles on panel B indicate all known presence points collected from GBIF from 1990 to 2019, which corresponds to the current condition in our prediction. The occurrences of GBIFs are distributed inwith higher population fitness habitat ($\lambda > 1$), confirming that our study approach can reasonably predict range shifts.

²⁹⁹ **Discussion**

300 **References**

- 301 Bertrand, R., Lenoir, J., Piedallu, C., Riofrío-Dillon, G., De Ruffray, P., Vidal, C., Pierrat, J.-C.,
302 and Gégout, J.-C. (2011). Changes in plant community composition lag behind climate
303 warming in lowland forests. *Nature*, 479(7374):517–520.
- 304 Caswell, H. (1989). Analysis of life table response experiments i. decomposition of effects
305 on population growth rate. *Ecological Modelling*, 46(3-4):221–237.
- 306 Caswell, H. (2000). *Matrix population models*, volume 1. Sinauer Sunderland, MA.
- 307 Compagnoni, A., Steigman, K., and Miller, T. E. (2017). Can't live with them, can't live
308 without them? balancing mating and competition in two-sex populations. *Proceedings of*
309 *the Royal Society B: Biological Sciences*, 284(1865):20171999.
- 310 Czachura, K. and Miller, T. E. (2020). Demographic back-casting reveals that subtle
311 dimensions of climate change have strong effects on population viability. *Journal of Ecology*,
312 108(6):2557–2570.
- 313 Dahlgren, J. P., Bengtsson, K., and Ehrlén, J. (2016). The demography of climate-driven and
314 density-regulated population dynamics in a perennial plant. *Ecology*, 97(4):899–907.
- 315 Davis, M. B. and Shaw, R. G. (2001). Range shifts and adaptive responses to quaternary
316 climate change. *Science*, 292(5517):673–679.
- 317 Diez, J. M., Giladi, I., Warren, R., and Pulliam, H. R. (2014). Probabilistic and spatially variable
318 niches inferred from demography. *Journal of ecology*, 102(2):544–554.
- 319 Eberhart-Phillips, L. J., Küpper, C., Miller, T. E., Cruz-López, M., Maher, K. H., Dos Remedios,
320 N., Stoffel, M. A., Hoffman, J. I., Krüger, O., and Székely, T. (2017). Sex-specific early
321 survival drives adult sex ratio bias in snowy plovers and impacts mating system and
322 population growth. *Proceedings of the National Academy of Sciences*, 114(27):E5474–E5481.
- 323 Ellis, R. P., Davison, W., Queirós, A. M., Kroeker, K. J., Calosi, P., Dupont, S., Spicer, J. I.,
324 Wilson, R. W., Widdicombe, S., and Urbina, M. A. (2017). Does sex really matter? explaining
325 intraspecies variation in ocean acidification responses. *Biology letters*, 13(2):20160761.
- 326 Ellner, S. P., Childs, D. Z., Rees, M., et al. (2016). Data-driven modelling of structured
327 populations. *A practical guide to the Integral Projection Model*. Cham: Springer.

- 328 Evans, M. E., Merow, C., Record, S., McMahon, S. M., and Enquist, B. J. (2016). Towards
329 process-based range modeling of many species. *Trends in Ecology & Evolution*, 31(11):860–871.
- 330 Gamelon, M., Grøtan, V., Nilsson, A. L., Engen, S., Hurrell, J. W., Jerstad, K., Phillips, A. S.,
331 Røstad, O. W., Slagsvold, T., Walseng, B., et al. (2017). Interactions between demography
332 and environmental effects are important determinants of population dynamics. *Science
333 Advances*, 3(2):e1602298.
- 334 Gissi, E., Schiebinger, L., Hadly, E. A., Crowder, L. B., Santoleri, R., and Micheli, F. (2023).
335 Exploring climate-induced sex-based differences in aquatic and terrestrial ecosystems to
336 mitigate biodiversity loss. *nature communications*, 14(1):4787.
- 337 Hernández, C. M., Ellner, S. P., Adler, P. B., Hooker, G., and Snyder, R. E. (2023). An exact
338 version of life table response experiment analysis, and the r package exactltre. *Methods
339 in Ecology and Evolution*, 14(3):939–951.
- 340 Hitchcock, A. S. (1971). *Manual of the grasses of the United States*, volume 2. Courier Corporation.
- 341 Iler, A. M., Compagnoni, A., Inouye, D. W., Williams, J. L., CaraDonna, P. J., Anderson, A., and
342 Miller, T. E. (2019). Reproductive losses due to climate change-induced earlier flowering are
343 not the primary threat to plant population viability in a perennial herb. *Journal of Ecology*,
344 107(4):1931–1943.
- 345 Jones, M. H., Macdonald, S. E., and Henry, G. H. (1999). Sex-and habitat-specific responses
346 of a high arctic willow, *salix arctica*, to experimental climate change. *Oikos*, pages 129–138.
- 347 Karger, D. N., Conrad, O., Böhner, J., Kawohl, T., Kreft, H., Soria-Auza, R. W., Zimmermann,
348 N. E., Linder, H. P., and Kessler, M. (2017). Climatologies at high resolution for the earth’s
349 land surface areas. *Scientific data*, 4(1):1–20.
- 350 Kindiger, B. (2004). Interspecific hybrids of *poa arachnifera* × *poa secunda*. *Journal of New
351 Seeds*, 6(1):1–26.
- 352 Lee-Yaw, J. A., Kharouba, H. M., Bontrager, M., Mahony, C., Csergő, A. M., Noreen, A. M.,
353 Li, Q., Schuster, R., and Angert, A. L. (2016). A synthesis of transplant experiments and
354 ecological niche models suggests that range limits are often niche limits. *Ecology letters*,
355 19(6):710–722.
- 356 Leicht-Young, S. A., Silander, J. A., and Latimer, A. M. (2007). Comparative performance of
357 invasive and native *celastrus* species across environmental gradients. *Oecologia*, 154:273–282.

- 358 Liaw, A., Wiener, M., et al. (2002). Classification and regression by randomforest. *R news*,
359 2(3):18–22.
- 360 Louthan, A. M., Keighron, M., Kiekebusch, E., Cayton, H., Terando, A., and Morris, W. F.
361 (2022). Climate change weakens the impact of disturbance interval on the growth rate of
362 natural populations of venus flytrap. *Ecological Monographs*, 92(4):e1528.
- 363 Merow, C., Bois, S. T., Allen, J. M., Xie, Y., and Silander Jr, J. A. (2017). Climate change both
364 facilitates and inhibits invasive plant ranges in new england. *Proceedings of the National
365 Academy of Sciences*, 114(16):E3276–E3284.
- 366 Miller, T. and Compagnoni, A. (2022a). Data from: Two-sex demography, sexual niche
367 differentiation, and the geographic range limits of texas bluegrass (*Poa arachnifera*). *American
368 Naturalist, Dryad Digital Repository*. <https://doi.org/10.5061/dryad.kkwh70s5x>.
- 369 Miller, T. E. and Compagnoni, A. (2022b). Two-sex demography, sexual niche differentiation,
370 and the geographic range limits of texas bluegrass (*poa arachnifera*). *The American
371 Naturalist*, 200(1):17–31.
- 372 Morrison, C. A., Robinson, R. A., Clark, J. A., and Gill, J. A. (2016). Causes and consequences
373 of spatial variation in sex ratios in a declining bird species. *Journal of Animal Ecology*,
374 85(5):1298–1306.
- 375 Morrison, S. F. and Hik, D. S. (2007). Demographic analysis of a declining pika *ochotona
376 collaris* population: linking survival to broad-scale climate patterns via spring snowmelt
377 patterns. *Journal of Animal ecology*, pages 899–907.
- 378 O'Connell, R. D., Doak, D. F., Horvitz, C. C., Pascarella, J. B., and Morris, W. F. (2024). Nonlinear
379 life table response experiment analysis: Decomposing nonlinear and nonadditive population
380 growth responses to changes in environmental drivers. *Ecology Letters*, 27(3):e14417.
- 381 Pease, C. M., Lande, R., and Bull, J. (1989). A model of population growth, dispersal and
382 evolution in a changing environment. *Ecology*, 70(6):1657–1664.
- 383 Petry, W. K., Soule, J. D., Iler, A. M., Chicas-Mosier, A., Inouye, D. W., Miller, T. E., and
384 Mooney, K. A. (2016). Sex-specific responses to climate change in plants alter population
385 sex ratio and performance. *Science*, 353(6294):69–71.
- 386 Piironen, J. and Vehtari, A. (2017). Comparison of bayesian predictive methods for model
387 selection. *Statistics and Computing*, 27:711–735.

- 388 Pottier, P., Burke, S., Drobniak, S. M., Lagisz, M., and Nakagawa, S. (2021). Sexual (in) equality?
389 a meta-analysis of sex differences in thermal acclimation capacity across ectotherms.
390 *Functional Ecology*, 35(12):2663–2678.
- 391 R Core Team (2023). *R: A Language and Environment for Statistical Computing*. R Foundation
392 for Statistical Computing, Vienna, Austria.
- 393 Sanderson, B. M., Knutti, R., and Caldwell, P. (2015). A representative democracy to reduce
394 interdependency in a multimodel ensemble. *Journal of Climate*, 28(13):5171–5194.
- 395 Schwalm, C. R., Glendon, S., and Duffy, P. B. (2020). Rcp8. 5 tracks cumulative co2 emissions.
396 *Proceedings of the National Academy of Sciences*, 117(33):19656–19657.
- 397 Schwinning, S., Lortie, C. J., Esque, T. C., and DeFalco, L. A. (2022). What common-garden
398 experiments tell us about climate responses in plants.
- 399 Sexton, J. P., McIntyre, P. J., Angert, A. L., and Rice, K. J. (2009). Evolution and ecology of
400 species range limits. *Annu. Rev. Ecol. Evol. Syst.*, 40:415–436.
- 401 Smith, M. D., Wilkins, K. D., Holdrege, M. C., Wilfahrt, P., Collins, S. L., Knapp, A. K., Sala,
402 O. E., Dukes, J. S., Phillips, R. P., Yahdjian, L., et al. (2024). Extreme drought impacts have
403 been underestimated in grasslands and shrublands globally. *Proceedings of the National
404 Academy of Sciences*, 121(4):e2309881120.
- 405 Stan Development Team (2023). RStan: the R interface to Stan. R package version 2.21.8.
- 406 Thomson, A. M., Calvin, K. V., Smith, S. J., Kyle, G. P., Volke, A., Patel, P., Delgado-Arias,
407 S., Bond-Lamberty, B., Wise, M. A., Clarke, L. E., et al. (2011). Rcp4. 5: a pathway for
408 stabilization of radiative forcing by 2100. *Climatic change*, 109:77–94.
- 409 Tognetti, R. (2012). Adaptation to climate change of dioecious plants: does gender balance
410 matter? *Tree Physiology*, 32(11):1321–1324.

Supporting Information

411 S.1 XX

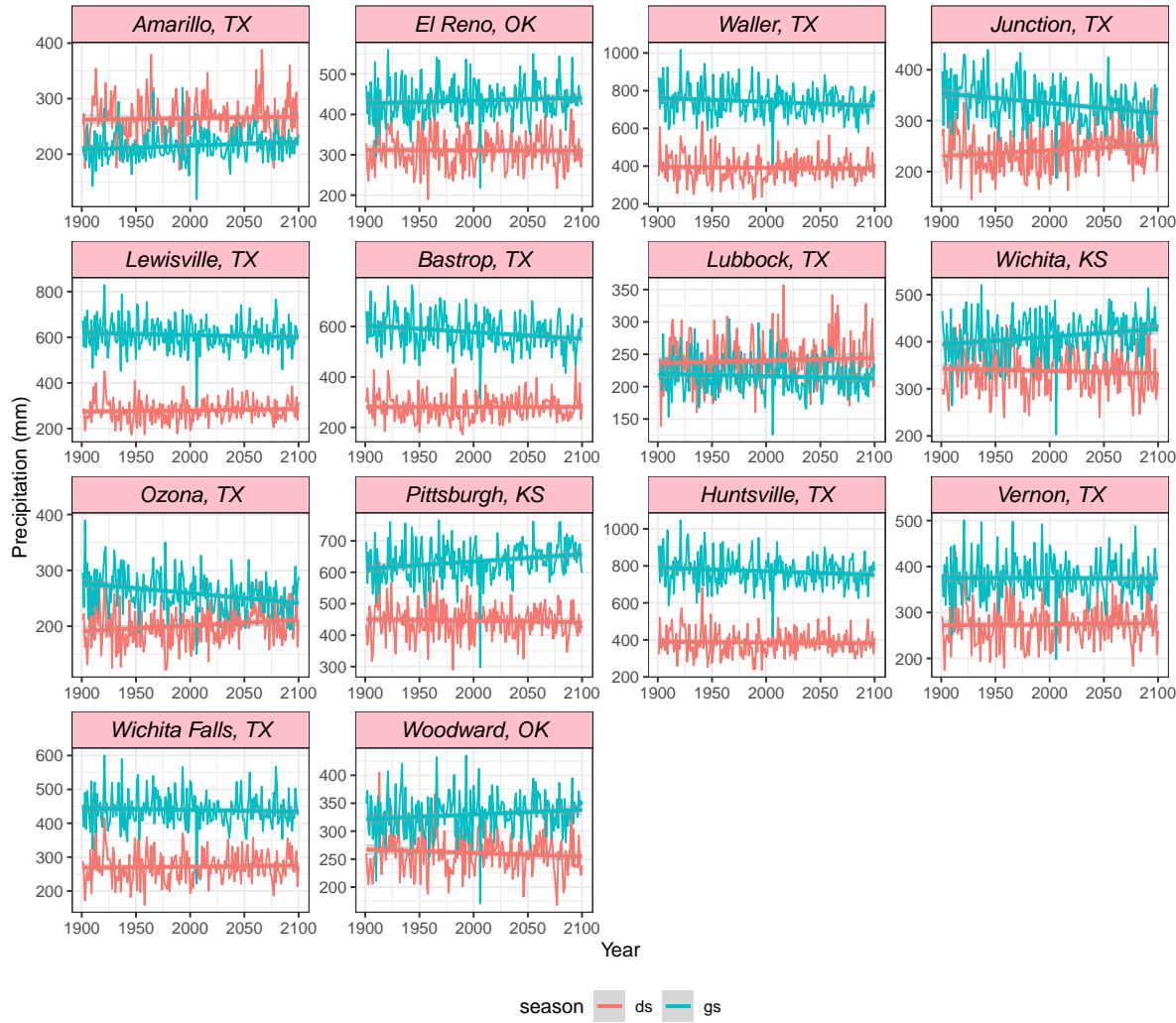


Figure S-1: Precipitation variation across the study sites from 1990 to 2100

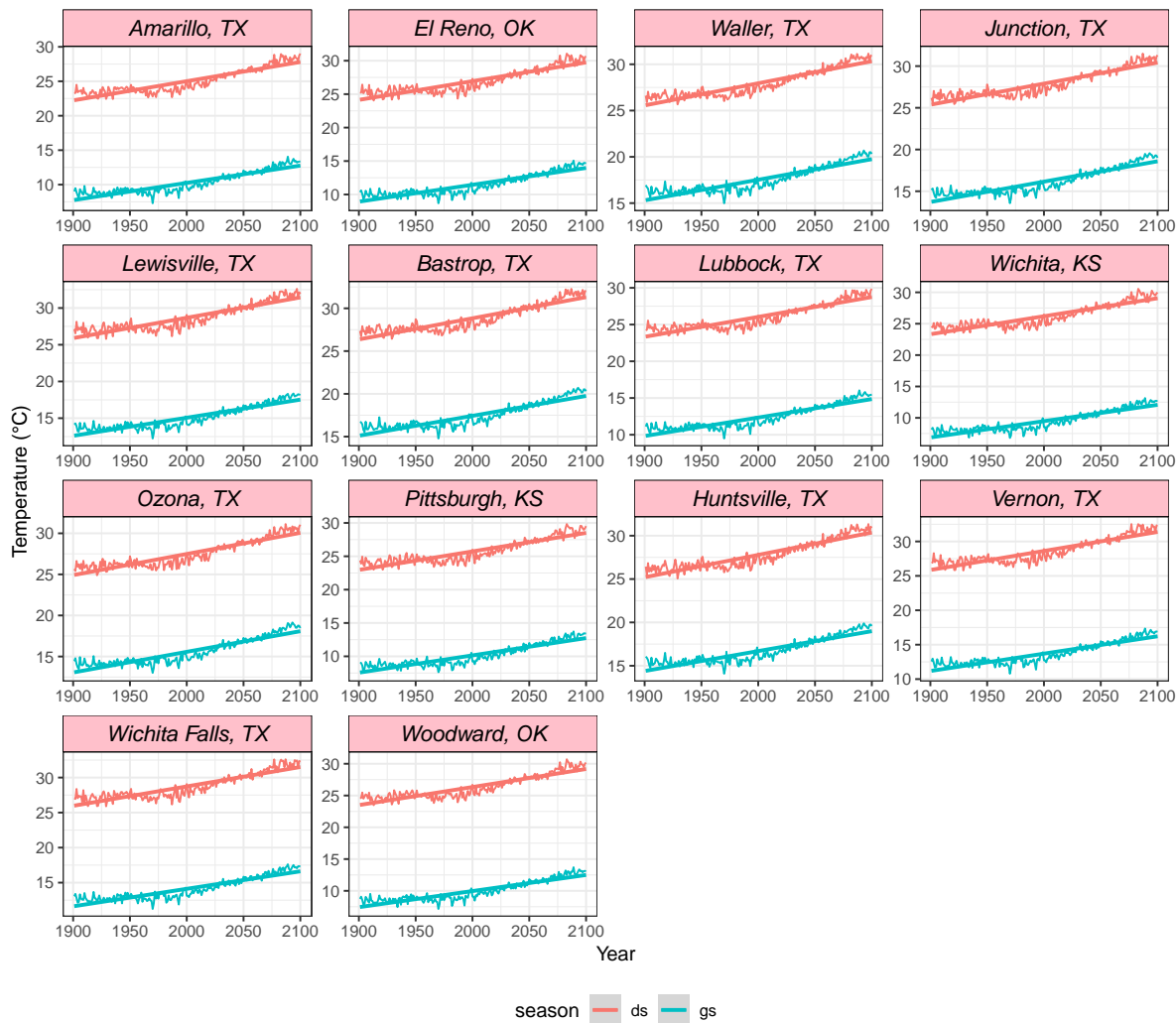


Figure S-2: Temperature variation across the study sites from 1990 to 2100

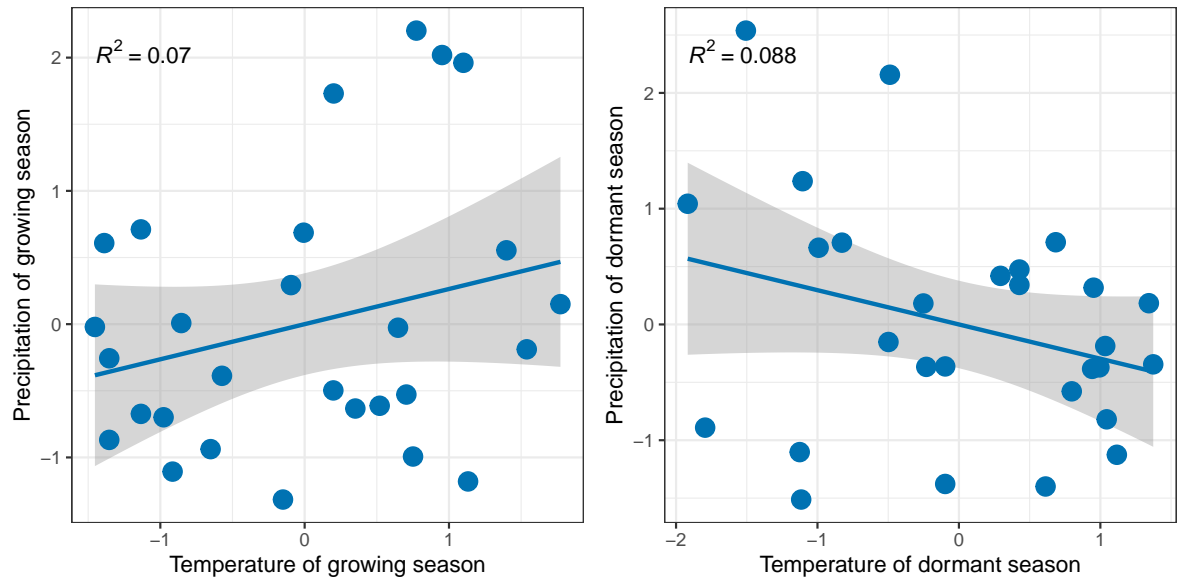


Figure S-3: Relation between precipitation and temperature for each season (growing and dormant). R^2 indicates the value of proportion of explained variance between the temperature and precipitation

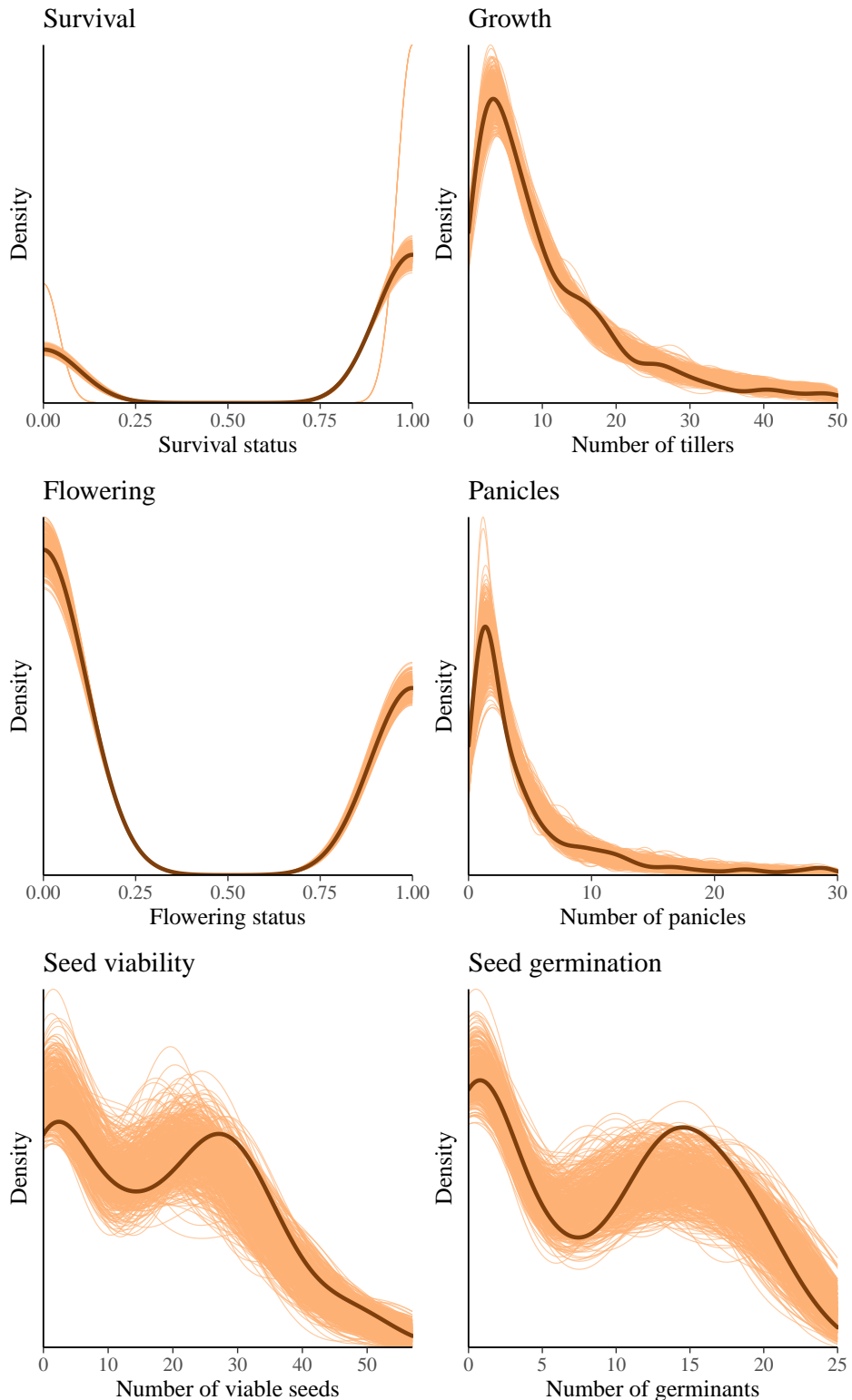


Figure S-4: Consistency between real data and simulated values suggests that the fitted model accurately describes the data. Graph shows density curves for the observed data (light blue) along with the simulated values (dark blue). The first column shows the linear models and the second column shows the 2 degree polynomial models.

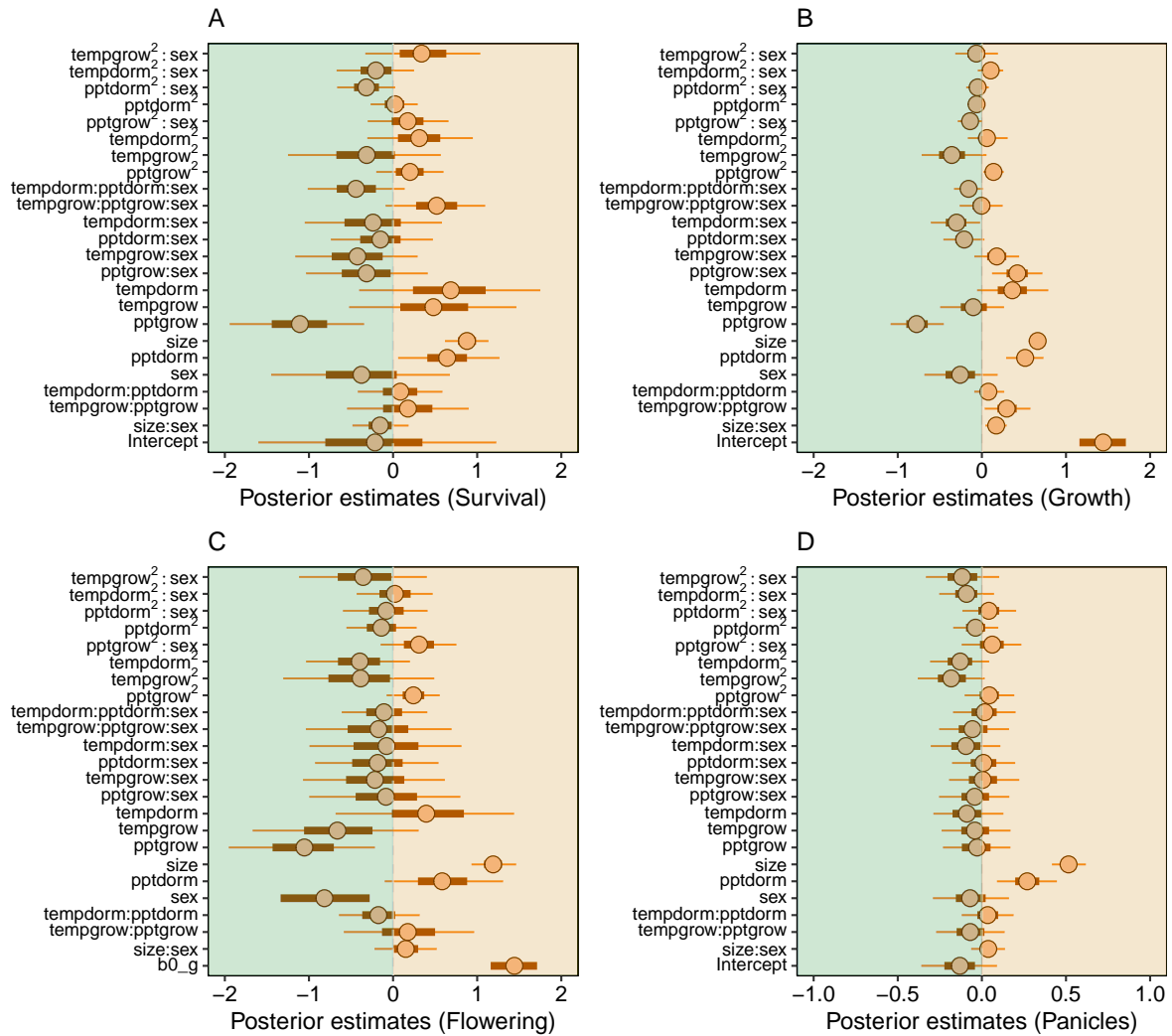


Figure S-5: Mean parameter values and 95% credible intervals for all vital rates.

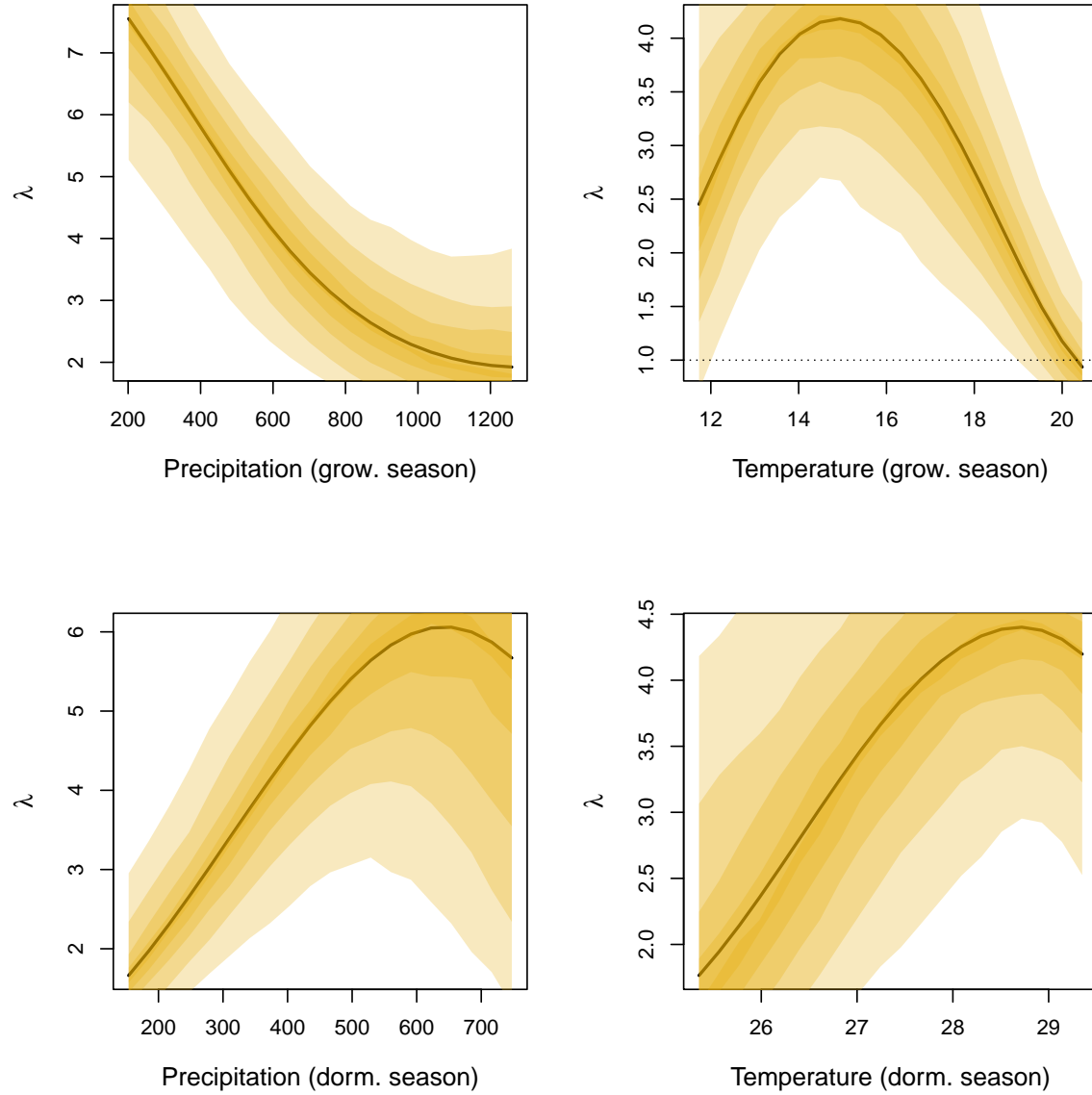


Figure S-6: Population growth rate (λ) as a function of seasonal climate (2016-2017), predicted by the two-sex matrix projection model that incorporates sex-specific demographic responses to climate with sex ratio-dependent seed fertilization. We show the mean posterior distribution of λ in solid lines, and the 5, 25, 50, 75, and 95% percentiles of parameter uncertainty in shaded gold color. The dashed horizontal line indicates the limit of population viability ($\lambda = 1$)

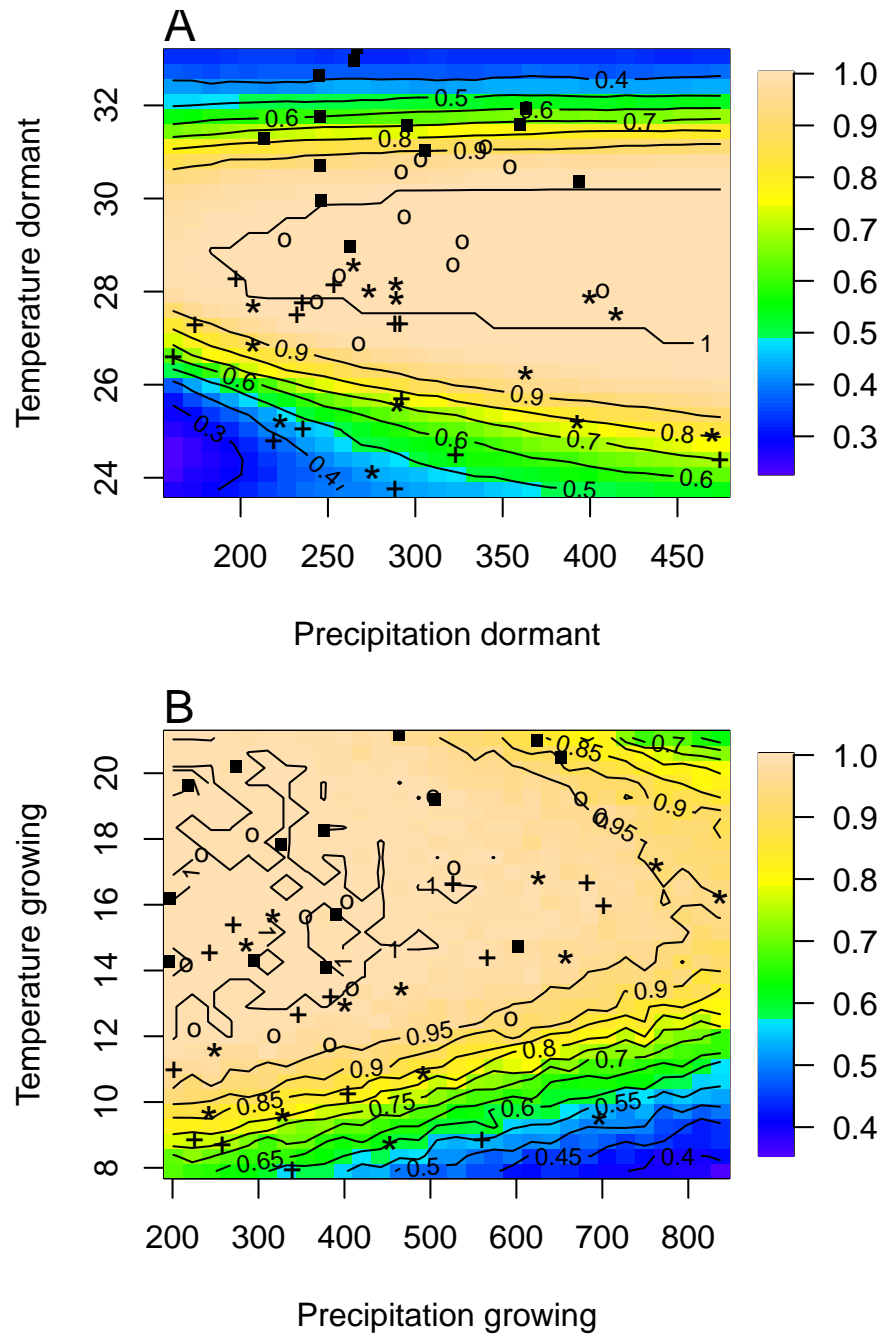


Figure S-7: Predicted niche shift for past, present and future climate conditions based on $\text{Pr} (\lambda \geq 1)$. Niche of dormant season (A), Niche of growing season (B). Contours show predicted probabilities of self-sustaining populations $\text{Pr} (\lambda \geq 1)$ conditional on precipitation and temperature of the dormant and growing season."+" Past, "*" Current,"o" RCP 45, ." RCP 85

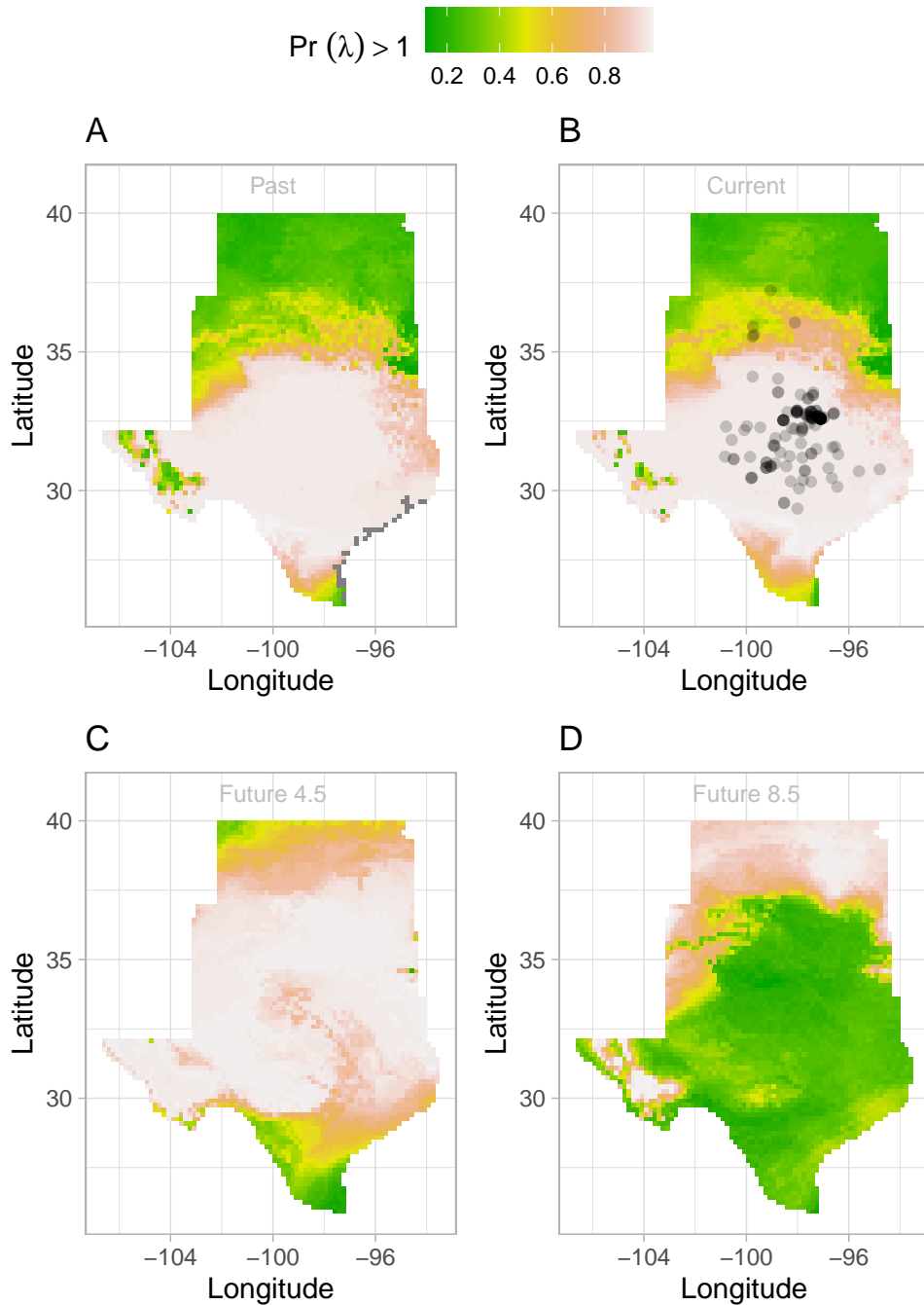


Figure S-8: Past (A), Current (B), Future CMCM (2070–20100) (C and D) predicted range shift based on population growth rate. Future projections were based on the average population growth rate in four GCMs. The black circles on panel B indicate all known presence points collected from GBIF from 1990 to 2019, which corresponds to the current condition in our prediction. The occurrences of GBIFs are distributed inwith higher population fitness habitat ($\lambda > 1$) , confirming that our study approach can reasonably predict range shifts.

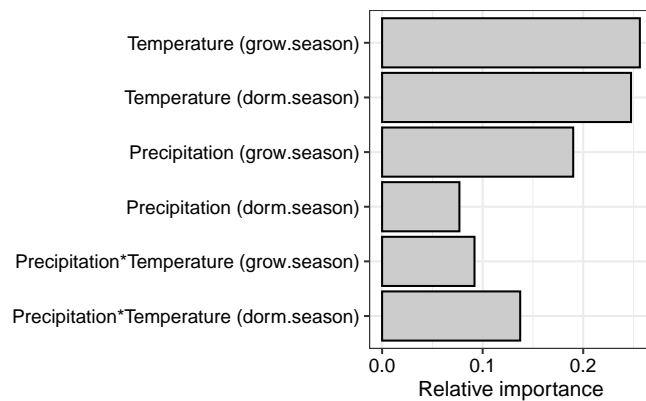


Figure S-9: XXX